

VIEWPOINT MATTERS: DYNAMICALLY OPTIMIZING VIEWPOINTS WITH MASKED AUTOENCODER FOR VISUAL MANIPULATION

Pengfei Yi¹, Yifan Han¹, Junyan Li¹, Litao Liu³, and Wenzhao Lian^{2†}

¹Institute of Automation, Chinese Academy of Sciences

²School of Artificial Intelligence, Shanghai Jiao Tong University, ³Rutgers University

ABSTRACT

Robotic manipulation continues to be a challenge, and imitation learning (IL) enables robots to learn tasks from expert demonstrations. Current IL methods typically rely on fixed camera setups, where cameras are manually positioned in static locations, imposing significant limitations on adaptability and coverage. Inspired by human active perception, where humans dynamically adjust their viewpoint to capture the most relevant and least noisy information, we propose MAE-Select, a novel framework for active viewpoint selection in single-camera robotic systems. MAE-Select fully leverages pre-trained multi-view masked autoencoder representations and dynamically selects the next most informative viewpoint at each time chunk without requiring labeled viewpoints. Extensive experiments demonstrate that MAE-Select improves the capabilities of single-camera systems and, in some cases, even surpasses multi-camera setups. The project will be available at <https://mae-select.github.io>.

Index Terms— Manipulation, Imitation Learning, Active Perception

1. INTRODUCTION

Robotic manipulation is a core challenge in robotics. Imitation Learning (IL) [1, 2, 3, 4, 5] has become a leading approach for enabling robots to learn complex tasks through expert demonstrations. Recently, advances in deep generative models [6, 7, 8, 9], have empowered IL by allowing robots to process high-dimensional sensory inputs, leading to promising results in robotic manipulation [10, 11, 12, 13].

However, most current IL methods rely on fixed camera setups, either single or multiple cameras, which pose significant limitations. In fixed single-camera setups [14, 15], though cost-effective, robots face challenges due to the limited field of view, which may obstruct critical parts of the environments, negatively impacting task performance. Multi-camera setups, while designed to provide more comprehensive scene coverage, introduce their own complexities: the abundance of redundant or irrelevant information can overwhelm learning algorithms and decrease efficiency. As shown in Sec.3, these passive static multi-view setups do not always

provide the most task-relevant and cleanest information, leading to suboptimal decision-making.

In contrast, humans dynamically adjust their viewpoints while performing tasks. By actively moving our head, we naturally seek the most informative, least noisy perspectives. Inspired by this human capability, we propose shifting from passive, static perception to **active perception**, where the viewpoint is dynamically adjusted throughout the task to optimize information intake. In a practical robotic setting, this could be embodied by a robot moving its head to capture the most task-relevant views in real-time. In this paper, we focus on the feasibility of active viewpoint selection for robotic manipulation as an initial exploration along this direction.

To this end, we introduce **MAE-Select**, a framework designed to actively select optimal viewpoints for single-camera robotic setups. MAE-Select first fully utilizes the powerful pre-trained representations from the multi-view masked autoencoders (MAEs) [16, 17], leveraging its complete encoder-decoder architecture to obtain estimated multi-view representations. Unlike prior works that focus on fixed viewpoints [18], MAE-Select dynamically predicts the next better viewpoint based on the current chunk of visual and action information. Crucially, this viewpoint selection is learned solely through imitation learning, which does not require manual labels for optimal views. It demonstrates significant potential in the advancement of single-camera robotic manipulation.

Our key contributions are as follows:

- We propose MAE-Select, a novel mechanism that dynamically selects the next optimal viewpoint at each time chunk without manual labels.
- We present an IL framework that fully exploits pre-trained MAE representations for manipulation.
- We demonstrate through various experiments that MAE-Select enhances manipulation accuracy in single-camera setups, even outperforming multi-camera systems in certain tasks.

2. METHOD

We introduce **MAE-Select**, a novel framework that enables robotic agents to actively select informative viewpoints for

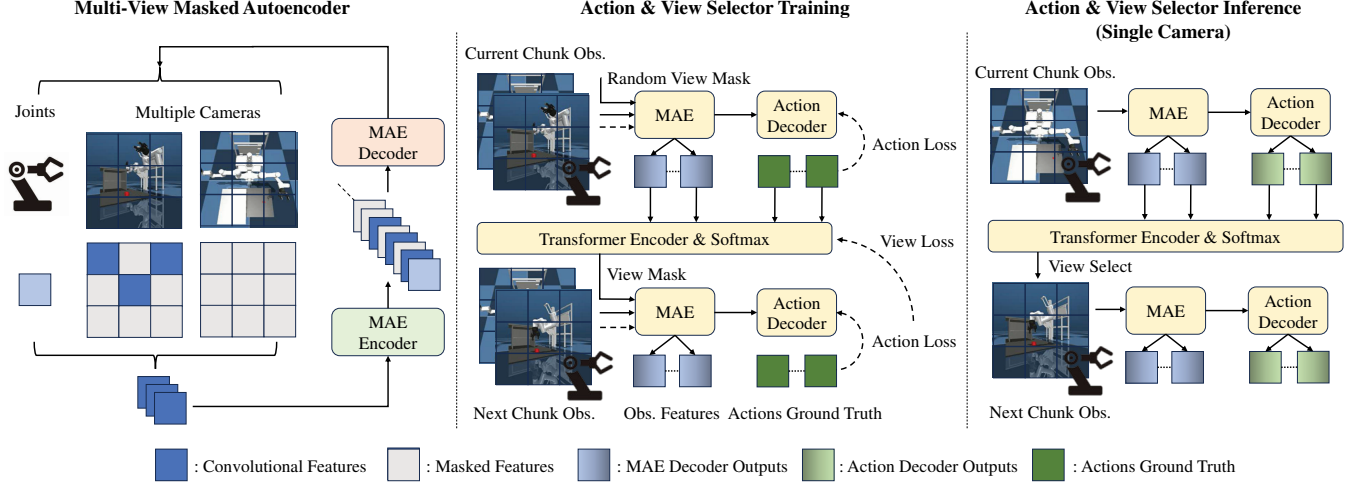


Fig. 1. Illustration of our proposed method. **Left** depicts the pre-training stage of the multi-view masked autoencoder with joint embeddings. **Middle** illustrates the training process of our framework using imitation learning. **Right** demonstrates how the framework operates during inference.

manipulation tasks. The core of our approach is a new formulation in which optimal viewpoint selection is learned implicitly through an imitation learning objective, without requiring explicit supervision or reinforcement learning. Unlike previous work that only uses pre-trained encoders [19, 18], our method exploits both encoder and decoder of a multiview masked autoencoder (MV-MAE), enabling the agent to construct a rich scene representation from a single view, crucial for accurate action prediction and informed viewpoint selection. An overview of our architecture is shown in Fig. 1.

2.1. Problem Formulation

We frame the robotic manipulation task as a learning problem over a sequence of observations and actions. Let the agent’s state at time t be composed of its proprioceptive information s_t (e.g., joint angles) and a set of visual observations $O_t = \{o_t^v\}_{v \in V}$ from a fixed set of N_v available viewpoints V . The agent’s goal is to learn a policy π that takes the current state and generates a chunk of T future actions, $a_{t:T-1} = \{a_t, \dots, a_{t+T-1}\}$.

In our active perception setting, the policy does not have access to all viewpoints simultaneously. Instead, it operates on a single selected viewpoint $o_t^{v_t}$ at time t . Therefore, the objective is to learn two key policies:

1. **An action policy** $\pi_\theta(a_{t:T-1}|o_t^{v_t}, s_t)$: This policy predicts a sequence of future actions based on the current single-view observation and proprioceptive state.
2. **A view selection policy** $\pi_\psi(v_{t+T}|o_t^{v_t}, s_t, a_{t:T-1})$: This policy selects the most advantageous viewpoint, v_{t+T} , for the subsequent time chunk, conditioned on the information from the current chunk.

Both policies, parameterized by θ and ψ respectively, are

trained jointly from a dataset of expert demonstrations $\mathcal{D} = \{(O_t, s_t, a_t)\}_{t=0 \dots T_m}^N$ using an imitation learning framework.

2.2. Multi-View Masked Autoencoder Pre-training

We pre-train a Multi-View Masked Autoencoder (MV-MAE) on demonstration data to learn a compact, 3D-aware scene representation (Fig. 1, left).

Given a multi-view observation O_t , we extract feature maps $\{\bar{o}_t^v\}_{v \in V}$ and apply dual masking: (1) *patch masking*, which randomly masks a large portion of patches within each view, and (2) *view masking*, which randomly drops entire views to encourage cross-view reasoning. The remaining patches, with view and position embeddings, are fed into a Transformer encoder f_ϕ to produce latent z_t^m . A decoder g_ϕ reconstructs all views from z_t^m , mask tokens, and the robot state embedding s_t by minimizing

$$\mathcal{L}_{\text{MAE}} = \mathbb{E}_{O_t, s_t} [\|O_t - g_\phi(f_\phi(O_t^m), s_t)\|_2^2]. \quad (1)$$

This pre-training enables the model to infer full 3D scenes from partial or occluded inputs for downstream tasks.

2.3. Next Better Viewpoint Selection

Following pre-training, we jointly fine-tune the model and train both the action and viewpoint selection policies (Fig. 1, middle). Although action decoder training uses ground-truth actions, defining a ground-truth “optimal” viewpoint is impractical, as it depends on task and context. Instead of reinforcement learning, which is difficult due to the sim-to-real gap, we propose a label-free strategy to train the viewpoint selector π_ψ . Specifically, the action prediction loss on a future data chunk \mathcal{D}_{t+T} is used as a supervisory signal for the viewpoint chosen in the current chunk \mathcal{D}_t . We apply this process to two consecutive trajectory chunks, \mathcal{D}_t and \mathcal{D}_{t+T} .

Processing the Current Chunk (\mathcal{D}_t): For the current chunk starting at time t , we begin with a single view o_t^v , selected uniformly at random. This single-view observation is passed through the entire pre-trained MV-MAE (f_ϕ, g_ϕ) to generate an estimated multi-view feature context $C_t = g_\phi(f_\phi(o_t^v), s_t)$. This context C_t is then fed into the action decoder π_θ , a diffusion-based policy, which is trained to predict the noise ϵ_t added to the expert action trajectory $a_{t:t+T-1}$. The action loss for this chunk is computed as:

$$\mathcal{L}_{\text{action}}^{(t)} = \mathbb{E}_{\epsilon_t, k} [\|\epsilon_t - \pi_\theta(C_t, a_{t:t+T-1}^0 + \epsilon_t, k)\|^2] \quad (2)$$

where $k \sim \mathcal{U}(1, K)$ is a randomly sampled diffusion timestep.

Selecting the View for the Next Chunk (\mathcal{D}_{t+T}): The viewpoint selector π_ψ , implemented as a Transformer encoder, takes the feature context C_t and the ground-truth action trajectory $a_{t:t+T-1}$ from the current chunk to predict a probability distribution of viewpoints for the next chunk:

$$\hat{c} = \text{Softmax}(\pi_\psi(C_t, a_{t:t+T-1})) \quad (3)$$

To select a viewpoint while maintaining differentiability for backpropagation, we employ a straight-through estimator as VQ-VAE [20]. In the forward, we perform an argmax operation to obtain one-hot vector y representing the chosen view. For the backward, gradients flow through the continuous softmax probabilities \hat{c} . This is implemented as:

$$y = \hat{c} + sg[(y - \hat{c})] \quad (4)$$

where $sg[\cdot]$ denotes the stop-gradient operator. This mechanism enables the gradient from the subsequent action loss to inform the selection policy.

Processing the Next Chunk (\mathcal{D}_{t+T}): The one-hot vector y is used to select a single viewpoint $o_{t+T}^{\hat{v}}$ from the next observation set O_{t+T} . This selection is performed via a dot product $o_{t+T}^{\hat{v}} = y \cdot O_{t+T}$, which also enables gradient flow back to the selection policy. This selected view is then processed through the identical pipeline as the first chunk, yielding a corresponding action loss, $\mathcal{L}_{\text{action}}^{(t+T)}$.

Updating the Viewpoint Selector: There is no explicit “view loss.” The viewpoint selector π_ψ is trained using gradients from the future action loss $\mathcal{L}_{\text{action}}^{(t+T)}$, backpropagated through the action decoder and selected observation via STE, directly optimizing π_ψ to select viewpoints that minimize future action prediction error.

The overall objective combines both action losses and the auxiliary reconstruction loss:

$$\mathcal{L}_{\text{total}} = \mathcal{L}_{\text{action}}^{(t)} + \lambda_1 \mathcal{L}_{\text{action}}^{(t+T)} + \lambda_2 \mathcal{L}_{\text{MAE}} \quad (5)$$

where π_θ is updated by both action losses, while π_ψ is optimized only by the future action loss.

Inference: During inference (Fig. 1, right), the process is autoregressive. Starting from a random initial viewpoint, it

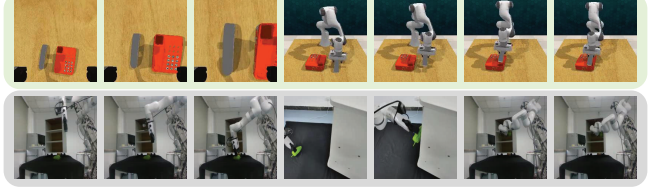


Fig. 2. Visualization of the selected viewpoints in our experiments, showcasing both simulation and real-world environments. Each row represents the procedure of a specific task, indicating the necessity of selecting different viewpoints.

predicts both the current action chunk and the optimal viewpoint for the next chunk. The predicted action is then used alongside the newly selected viewpoint for the subsequent step, creating a dynamic perception-action loop.

3. EXPERIMENTS

We evaluate MAE-Select across 3 challenging scenarios and 8 demanding tasks in simulation, including simulations in ACT [11], RLBench [21], and our designed robot in MuJoCo [22], along with three real-world tasks.

3.1. Implementation

We explore a single-camera control setup where the system is trained with multiple camera views but deployed with a single moving camera. At each time chunk, the camera is placed at one of the training viewpoints, enabling flexible operation in real-world settings where only one camera is available. We base our implementation on the architecture of the diffusion policy [10]. The action space corresponds to the joint angles of the robot arm, while the image observations have a resolution of 224×224 with a patch size of 16. Our masked autoencoder utilizes a 12-layer ViT [23] for encoder and an 8-layer ViT for decoder, with an embedding dimension of 512. During pretraining, we use a batch size of 128 over 100 epochs. For RLBench and real-world tasks, the time chunk size is set to 20, with a total of 600 epochs. For other tasks, the time chunk size is 100, with 1,000 epochs in total. λ_1 and λ_2 are empirically set to 2.0 and 1.0, respectively. For each method, we evaluate the best-performing checkpoints from the last three evaluated at 100-intervals, with 50 environment initializations in simulation. All models were trained and tested on NVIDIA RTX 4090 GPUs.

3.2. Results

We compare MAE-Select with Diffusion Policy [10] and its MAE-enhanced variant (MAE-Diffusion) across various tasks. Unlike the baselines, which use fixed viewpoints during training and testing, MAE-Select leverages multi-view training and dynamically selects the most informative single viewpoint for the next time chunk during inference.

Table 1. Results of comparison experiment. * represents with Disturbance. For the eight simulated tasks, we report the success rate, with 50 policy evaluations each. For the real-world tasks, we report the number of successes, training with human data, with 10 evaluations. For Diffusion Policy and MAE-Diffusion, the viewpoint data used for training is the same as the viewpoint used for testing. For MAE-Select, we use both viewpoints for training and only one viewpoint is used per time chunk during testing. Bold and underlined fonts mean the best and second-best results.

Method	Bimanual Insertion			Put Box In Cabinet			Put Box In Bin			Put Box In Bin*		
	Top	Front	Both	Top	Left	Both	Top	Left	Both	Top	Left	Both
Diffusion Policy [10]	42%	44%	50%	16%	18%	26%	80%	64%	84%	38%	30%	44%
MAE-Diffusion	48%	50%	54%	42%	42%	<u>46%</u>	84%	78%	92%	52%	46%	60%
MAE-Select			<u>52%</u>			50%			<u>88%</u>			<u>58%</u>
Method	Phone On Base			Pick Up Cup			Take Umbrella			Unplug Charger		
	Front	Wrist	Both	Front	Wrist	Both	Front	Wrist	Both	Top	Wrist	Both
Diffusion Policy [10]	82%	56%	78%	60%	40%	64%	58%	36%	54%	44%	30%	34%
MAE-Diffusion	86%	70%	<u>88%</u>	<u>68%</u>	66%	62%	56%	42%	64%	46%	34%	<u>52%</u>
MAE-Select			92%			70%			<u>60%</u>			58%
Method	Put Eggplant To Bowl			Put Eggplant To Bowl*			Put Bitter Melon In Cabinet					
	Top	Wrist	Both	Top	Wrist	Both	Top	Left	Both			
Diffusion Policy [10]	2/10		1/10	5/10	2/10	0/10	3/10	0/10	1/10			2/10
MAE-Diffusion	4/10		4/10	7/10	<u>4/10</u>	3/10	6/10	2/10	<u>4/10</u>			<u>4/10</u>
MAE-Select			<u>6/10</u>			6/10						5/10

Table 2. Results of ACT experiments. We report the success rate, with 50 policy evaluations each. Bold and underlined fonts mean the best and second-best results.

Method	Bimanual Insertion			Phone On Base		
	Top	Front	Both	Front	Wrist	Both
ACT	14%	26%	34%	56%	50%	58%
MAE-ACT	28%	30%	42%	60%	58%	<u>66%</u>
MAE-Select		<u>36%</u>			70%	

Table 3. Ablation Studies on MAE Encoder and Decoder Utilization.

Method	Put Box In Cabinet			Phone On Base		
	Top	Left	Both	Front	Wrist	Both
MAE-Encoder	20%	28%	34%	76%	56%	80%
MAE-Diffusion	42%	42%	46%	86%	70%	88%

As shown in Tab.1, MAE-Select consistently outperforms fixed single-camera setups in both simulation and real-world experiments—for instance, achieving an 8% gain over the best fixed camera method and 32% over prior work in the *Put Box In Cabinet* task. Its strength lies in intelligently exploiting limited visual input through optimal viewpoint selection. Interestingly, in some tasks a single camera even surpasses multi-camera setups (e.g., Diffusion Policy on *Unplug Charger*: top view 44% vs. two views 34%), likely due to noise and alignment issues from multiple inputs. MAE-Select avoids such pitfalls, remaining competitive and often superior, even compared with multi-camera configurations.

To analyze system behavior under single-camera control,

we visualize deployment phases (Fig.2). MAE-Select adaptively selects optimal viewpoints, focusing on critical regions while ignoring irrelevant areas.

3.3. Ablation Study

Our viewpoint selection method is agnostic to the choice of action decoder, as evidenced by its integration with ACT [11] (Tab.2), confirming its adaptability across architectures. We further conduct an ablation study comparing the full encoder-decoder masked autoencoder with a variant using only the encoder [19, 18]. Results (Tab.3) show that leveraging the full structure significantly boosts performance, especially under occlusion, highlighting the decoder’s role in refining visual representations and improving generalization in both simulation and real-world tasks.

4. CONCLUSIONS AND FUTURE WORK

We propose MAE-Select, a framework that enables single-camera robots to actively optimize viewpoints for manipulation tasks. By exploiting pre-trained multi-view masked autoencoder representations and dynamically selecting informative viewpoints at each time chunk without manual annotations, MAE-Select boosts manipulation efficiency and can even outperform multi-camera systems. Its main limitation is optimizing over discrete rather than continuous viewpoints, which limits flexibility in dynamic environments. Future work could integrate NeRF [24] or 3D Gaussian processes [25] for continuous viewpoint optimization.

5. REFERENCES

- [1] Dean A Pomerleau, “Alvinn: An autonomous land vehicle in a neural network,” *NeurIPS*, 1988.
- [2] Eric Jang, Alex Irpan, Mohi Khansari, Daniel Kappler, Frederik Ebert, Corey Lynch, Sergey Levine, and Chelsea Finn, “Bc-z: Zero-shot task generalization with robotic imitation learning,” in *CoRL*, 2022.
- [3] Pete Florence, Corey Lynch, Andy Zeng, Oscar A Ramirez, Ayzaan Wahid, Laura Downs, Adrian Wong, Johnny Lee, Igor Mordatch, and Jonathan Tompson, “Implicit behavioral cloning,” in *CoRL*, 2022.
- [4] Frederik Ebert, Yanlai Yang, Karl Schmeckpeper, Bernadette Bucher, Georgios Georgakis, Kostas Daniilidis, Chelsea Finn, and Sergey Levine, “Bridge data: Boosting generalization of robotic skills with cross-domain datasets,” *arXiv preprint*, 2021.
- [5] Anthony Brohan, Noah Brown, Justice Carbajal, Yevgen Chebotar, Joseph Dabis, Chelsea Finn, Keerthana Gopalakrishnan, Karol Hausman, Alex Herzog, Jasmine Hsu, et al., “Rt-1: Robotics transformer for real-world control at scale,” *arXiv preprint*, 2022.
- [6] Ian Goodfellow, Jean Pouget-Abadie, Mehdi Mirza, Bing Xu, David Warde-Farley, Sherjil Ozair, Aaron Courville, and Yoshua Bengio, “Generative adversarial networks,” *Communications of the ACM*, 2020.
- [7] Siyuan Huang, Zan Wang, Puhao Li, Baoxiong Jia, Tengyu Liu, Yixin Zhu, Wei Liang, and Song-Chun Zhu, “Diffusion-based generation, optimization, and planning in 3d scenes,” in *CVPR*, 2023.
- [8] Diederik P Kingma, “Auto-encoding variational bayes,” *arXiv preprint*, 2013.
- [9] Jonathan Ho, Ajay Jain, and Pieter Abbeel, “Denoising diffusion probabilistic models,” *NeurIPS*, 2020.
- [10] Cheng Chi, Siyuan Feng, Yilun Du, Zhenjia Xu, Eric Cousineau, Benjamin Burchfiel, and Shuran Song, “Diffusion policy: Visuomotor policy learning via action diffusion,” *RSS*, 2023.
- [11] Tony Z Zhao, Vikash Kumar, Sergey Levine, and Chelsea Finn, “Learning fine-grained bimanual manipulation with low-cost hardware,” *RSS*, 2023.
- [12] Homanga Bharadhwaj, Jay Vakil, Mohit Sharma, Abhinav Gupta, Shubham Tulsiani, and Vikash Kumar, “Roboagent: Generalization and efficiency in robot manipulation via semantic augmentations and action chunking,” in *ICRA*, 2024.
- [13] Moritz Reuss, Maximilian Li, Xiaogang Jia, and Rudolf Lioutikov, “Goal-conditioned imitation learning using score-based diffusion policies,” *arXiv preprint*, 2023.
- [14] Jyothish Pari, Nur Muhammad Shafiullah, Sridhar Pandian Arunachalam, and Lerrel Pinto, “The surprising effectiveness of representation learning for visual imitation,” *arXiv preprint*, 2021.
- [15] Yuzhe Qin, Hao Su, and Xiaolong Wang, “From one hand to multiple hands: Imitation learning for dexterous manipulation from single-camera teleoperation,” *IEEE RAL*, 2022.
- [16] Kaiming He, Xinlei Chen, Saining Xie, Yanghao Li, Piotr Dollár, and Ross Girshick, “Masked autoencoders are scalable vision learners,” in *CVPR*, 2022.
- [17] Zhan Tong, Yibing Song, Jue Wang, and Limin Wang, “Videomae: Masked autoencoders are data-efficient learners for self-supervised video pre-training,” *NeurIPS*, 2022.
- [18] Younggyo Seo, Junsu Kim, Stephen James, Kimin Lee, Jinwoo Shin, and Pieter Abbeel, “Multi-view masked world models for visual robotic manipulation,” in *ICML*, 2023.
- [19] Younggyo Seo, Danijar Hafner, Hao Liu, Fangchen Liu, Stephen James, Kimin Lee, and Pieter Abbeel, “Masked world models for visual control,” in *CoRL*, 2023.
- [20] Aaron Van Den Oord, Oriol Vinyals, et al., “Neural discrete representation learning,” *NeurIPS*, 2017.
- [21] Stephen James, Zicong Ma, David Rovick Arrojo, and Andrew J. Davison, “Rlbench: The robot learning benchmark & learning environment,” *IEEE RAL*, 2020.
- [22] Emanuel Todorov, Tom Erez, and Yuval Tassa, “MuJoCo: A physics engine for model-based control,” in *ICIRS*, 2012.
- [23] Alexey Dosovitskiy, “An image is worth 16x16 words: Transformers for image recognition at scale,” *arXiv preprint*, 2020.
- [24] Ben Mildenhall, Pratul P Srinivasan, Matthew Tancik, Jonathan T Barron, Ravi Ramamoorthi, and Ren Ng, “Nerf: Representing scenes as neural radiance fields for view synthesis,” *Communications of the ACM*, 2021.
- [25] Bernhard Kerbl, Georgios Kopanas, Thomas Leimkühler, and George Drettakis, “3d gaussian splatting for real-time radiance field rendering,” *ACM Trans. Graph.*, 2023.